

Evaluation of an HDPE geomembrane after 14 years as a leachate lagoon liner

R. Kerry Rowe, Henri P. Sangam, and Craig B. Lake

Abstract: A geomembrane – compacted clay composite liner system used to contain municipal solid waste (MSW) landfill leachate for 14 years is evaluated. Field observations of the geomembrane revealed many defects, including holes, patches, and cracks. Physical, chemical, and mechanical tests conducted on samples collected from five different locations of the liner suggest that samples continuously exposed to sunlight and high temperatures experienced more degradation compared to samples that were covered by leachate or soil. Sorption and diffusion tests revealed that the permeation coefficients of volatile organic compounds were in the range of 4×10^{-12} to 6×10^{-11} m²/s and that, with respect to these parameters, there was no significant difference between samples with different exposure levels. However, the permeation coefficients were between four and five times lower than values obtained for unaged HDPE geomembranes typical of present day production. Contaminant modelling of the entire lagoon liner suggests that the geomembrane liner most likely stopped being effective as a contaminant barrier to ionic species sometime between 0 and 4 years after the installation.

Key words: liquid containment, composite liner, diffusion, HDPE geomembrane, performance.

Résumé : On évalue un système de membrane étanche composite, comprenant une géomembrane et une couche d'argile compacte, utilisé pour confiner le lixiviat des enfouissements municipaux solides pour 14 ans. Des observations de la géomembrane sur le terrain ont révélé plusieurs défauts comprenant des trous, des pièces et des fissures. Des essais physiques, chimiques et mécaniques faits sur des échantillons prélevés de différentes positions sur la membrane suggèrent que les échantillons continuellement exposés aux rayons solaires et aux températures élevées ont subi plus de dégradations par rapport aux échantillons qui étaient couverts de lixiviat ou de sol. Des essais de sorption et de diffusion ont révélé que les coefficients de percolation des composés organiques volatiles étaient de l'ordre de 4×10^{-12} à 6×10^{-11} m²/s et que, en ce qui concerne ces paramètres, il n'y avait pas de différence significative entre les échantillons ayant différents niveaux d'exposition. Cependant, les coefficients de percolation étaient entre 4 à 5 fois plus faibles que les valeurs obtenues pour les géomembranes HDPE non vieilles typiques de la fabrication actuelle. La modélisation du contaminant de l'entière membrane étanche du bassin suggère que la géomembrane a arrêté très probablement d'être efficace comme barrière de contaminant aux espèces ioniques quelque part entre 0 à 4 ans après l'installation.

Mots clés : confinement de liquide, membrane composite, diffusion, géomembrane HDPE, performance.

[Traduit par la Rédaction]

Introduction

The use of a geomembrane in conjunction with compacted clay has been widely accepted as a composite liner system for modern landfills and wastewater lagoons (Rowe 2001). The level of understanding associated with the design, selection of materials, construction quality control, and long-term

protection of composite liners has improved considerably in recent years. The importance of some of these factors can best be illustrated with reference to case records. Because of the relatively short history of high-density polyethylene (HDPE) geomembrane usage in landfill applications, most of the reported case records are related to their use in liquid containment applications (Schmidt et al. 1984; Hsuan et al. 1991; Adams and Wagner 2000). Limited cases of HDPE geomembranes in landfill bottom liner applications found in the literature have been provided by Rollin et al. (1994) and Eith and Koerner (1997).

Issues regarding the hydraulic or diffusive performance of the geomembrane liner have not been directly addressed despite the fact that the primary function of a geomembrane is to act as a barrier against the migration of landfill leachate contaminants. Thus, the objective of this paper is to provide a case record based on the exhumation of a 14-year-old geomembrane from a leachate lagoon. Preliminary data for this particular case record was presented by Rowe et al. (1998). This investigation expands upon this preliminary in-

Received 3 January 2002. Accepted 20 January 2003.
Published on the NRC Research Press Web site at
<http://cgj.nrc.ca> on 1 May 2003.

R.K. Rowe¹ and **H.P. Sangam²** GeoEngineering Centre at Queen's–RMC, Department of Civil Engineering, Queen's University, Kingston, ON K7L 3N6, Canada.

C.B. Lake. Department of Civil Engineering, Dalhousie University, Sexton Campus, 1360 Barrington Street, Halifax, NS B3J 1Z1, Canada.

¹Corresponding author (e-mail: kerry@civil.queensu.ca).

²Present address: SNC-Lavalin Engineers & Constructors, 2200 Lake Shore Blvd., Toronto, ON M8V 1A4, Canada.

formation and examines (a) the difference in geomembrane properties that can arise from different exposure conditions, and (b) the influence of such exposure on the effectiveness of the geomembrane as a barrier to contaminant migration.

The lagoon

The leachate lagoon discussed in this study began to collect leachate in 1982 and was subsequently decommissioned after 14 years of service. Decommissioning was required to relocate the lagoon as part of ongoing landfill expansion. The lagoon was at a location in Ontario, Canada where the average temperatures during the winter and the summer were 1 and 25°C, respectively, and the latitude and longitude were 43°06'00"N and 79°04'00"W, respectively. The lagoon had a storage capacity of approximately 2500 m³ with side slopes of 3H:1V. It had been used to store leachate generated from a nonhazardous industrial, municipal, and commercial landfill. The leachate contained typical inorganic constituents, including transition and heavy metals (see Table 1). Volatile organic compounds were infrequently observed during the monitoring program, probably because of the nature of the waste in the landfill and (or) their volatilization during lagoon aeration.

The lagoon liner system consisted of a smooth 1.5 mm thick HDPE geomembrane overlying an approximately 3 m thick compacted clay liner constructed from "silty clay" borrow material obtained from near the landfill site. There was no protection layer above the geomembrane, which was directly exposed to the leachate and, above the leachate level, to the sunlight and the atmosphere. The original physical, chemical, and mechanical properties of the geomembrane and installation, as well as construction information, were not available to the authors. The hydrogeological conditions existing beneath the lagoon and on the site have been described by Lake (2000).

Field observations of the geomembrane and compacted clay liner

Geomembrane liner

After the lagoon was taken out of service, it was drained to examine the surface of the geomembrane. A significant amount of liquid at the bottom of the lagoon was trapped between the geomembrane and the clay giving the appearance of a "waterbed". An odorous black sludge was present at the bottom, especially near the influent pipe system. According to the landfill operators, the geomembrane component of the lagoon liner had a history of problems. During its lifespan, the lagoon had been drained several times to remove sludge and to patch geomembrane liner defects.

For investigation purposes, the exposed geomembrane liner was divided into five areas (north, east, south, and west side slopes and the bottom of the lagoon) with each of these five areas subdivided into 5 m × 5 m grid sections to map any features such as wrinkles, holes, cracks, and patches on the liner. Wrinkles were observed in the geomembrane at the top of the slopes of the lagoon, the diagonal intersection of side slopes, and at various locations on the bottom.

Detailed mapping of the liner revealed many defects (cracks, holes, and patches), as summarized in Table 2.

Table 1. Leachate characteristics from 1989 to 1995 (based on Gartner Lee Ltd., 1995).

Parameter	Mean concentration (mg/L)*
pH (–)	8.08
Conductivity (µs/cm)	15 200
Total dissolved solids (TDS)	11 300
Alkalinity	4 610
Hardness	1 040
Chemical oxygen demand (COD)	670
Biochemical oxygen demand (BOD)	200
Cl [–]	630
SO ₄ ^{2–}	3 110
Na ⁺	4 160
K ⁺	300
Mg ²⁺	150
NH ₃ -N	170
Al	140
Fe	1.3
Pb	3.3
Mn	0.025
Phenols	0.24

*Except as otherwise noted.

Cracks observed on the slopes where the HDPE geomembrane liner was not covered by the leachate and hence was exposed to the sunlight and climate extremes were typically oriented down the slope and located near either seams or patches. Figure 1 shows a typical crack located near the edge of a seam. The cracks observed at this site were similar to the field observations reported by Peggs and Carlson (1989) and Hsuan (1999) who attributed the cracks to high thermal contraction stresses along the top of the slope adjacent to the trench where the geomembrane is completely restrained from contraction. Some of these cracks were up to 30 cm long suggesting a high susceptibility of the geomembrane to cracking and hence the geomembrane as being relatively brittle. As shown in Table 2, four (19%) of the reported cracks were on the east, two (10%) on the west, eight (38%) on the north, and seven (33%) were on the south slope. No existing cracks were visible on the bottom. Of the cracks observed, only one was located below the leachate level.

Most of the holes recorded were located on the slope portion above the leachate level (see Table 2). However, in contrast to the cracks, the majority of the holes were found on the east side where the service way was located. A total of 54 patches (i.e., repaired former holes or cracks) were also observed on the liner (see Table 2). As with the other defects already mentioned, most of the patches (31 of 54) were found at the upper part of the liner. A few patches were observed at the bottom of the liner.

In summary, a total of 82 cracks, holes, and patches having different forms, patterns, and sizes were observed in the geomembrane over an area of 1552 m². This yields an average of 528 defects per hectare over the 14-year period of operation. Of these, 70% (348 defects per hectare) were above the leachate level and 30% (180 defects per hectare) were below the leachate level. Many scratches were also observed

Table 2. Distribution of defects (cracks, holes, and patches) on the geomembrane around the lagoon.

	Locations* (Area [†])					Total (1552 m ²)	Defects per hectare
	East (293 m ²)	West (289 m ²)	North (289 m ²)	South (291 m ²)	Bottom (390 m ²)		
Crack							
Slope above leachate level (148 m ²)	4	1	8	7	—	20	1351 [‡]
Slope below leachate level (1014 m ²)	0	1	0	0	—	1	10
Bottom (390 m ²)	—	—	—	—	0	0	0
Total cracks	4	2	8	7	0	21	
Cracks per hectare	136 [§]	69	277	241	0		135
Hole							
Slope above leachate level (148 m ²)	5	0	1	0	—	6	405
Slope below leachate level (1014 m ²)	0	1	0	0	—	1	10
Bottom (390 m ²)	—	—	—	—	0	0	0
Total holes	5	1	1	0	0	7	—
Holes per hectare	171	35	35	0	0	—	45
Patch							
Slope above leachate level (148 m ²)	17	4	5	5	—	31	2095
Slope below leachate level (1014 m ²)	5	4	5	3	—	17	168
Bottom (390 m ²)	—	—	—	—	6	6	154
Total patches	22	8	10	8	6	54	—
Patches per hectare	751	277	346	275	154	—	348

*The "north" slope faces south etc.

[†]Geomembrane area.

[‡]Formula $\frac{\text{Total cracks (20)}}{\text{Slope above leachate level (148 m}^2\text{)}}$.

[§]Formula $\frac{\text{Total cracks (4)}}{\text{Area East (293 m}^2\text{)}}$.

on the geomembrane at the bottom of the lagoon and may be attributable to either construction or maintenance activities during the service period of the facility.

Even though the majority (93%) of unrepaired cracks and holes were above the leachate level, the remaining cracks and (or) holes (7%) in the geomembrane along the side slopes appear to have been sufficient to allow liquid to get between the geomembrane and the clay liner. There were no cracks or holes found in the geomembrane at the bottom of the lagoon at the time of decommissioning, although 6 of the 54 patches were on the bottom.

Compacted clay liner

After examining the geomembrane portion of the lagoon liner, portions of it were removed to expose the underlying clay liner. It was observed that significant portions of the clay liner were desiccated above the leachate level. This phenomenon has been observed by others (Corser et al. 1992; Basnett and Brungard 1992). Below the leachate level, the clay appeared saturated and was covered by a thin layer of black sludge (~25 mm).

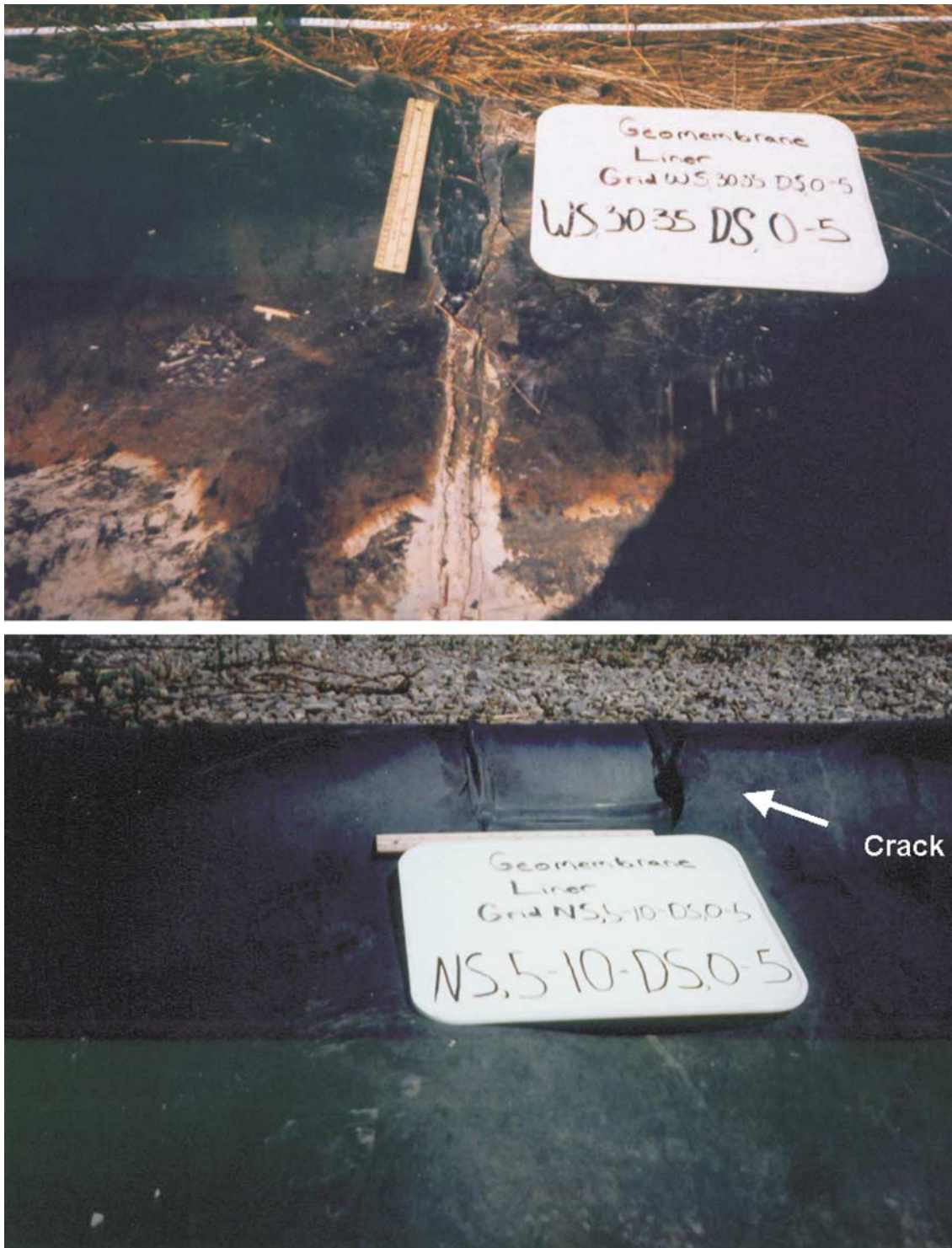
Five locations on the bottom of the lagoon were chosen for continuous borehole sampling. The details can be found in Lake (2000). The properties of the sampled clay material are summarized in Table 3. The water contents measured from samples taken from borehole samples ranged from 38% at the top of the compacted clay liner to about 20–24% at a depth of about 0.8 m. These latter water contents agree with unpublished construction reports that indicate that the clay liner was compacted at 2–4% wet of optimum with wa-

Table 3. Properties of compacted clay.

Physical parameters	
Relative density	2.68
Sand	Trace
Silt	63%
Clay	37%
Liquid limit	41%
Plastic limit	23%
Plastic index	18%
Activity	0.2
Water content	20–38%
Hydraulic conductivity	2×10^{-10} m/s
Mineral Composition	
Quartz	36%
K-Feldspar	4%
Na-Feldspar	5%
Calcite	18%
Dolomite	4%
Illite	20%
Chlorite	10%
Vermiculite	3%
Chemical Properties (on <75 µm fraction)	
Total organic carbon (TOC)	0.2%
pH	8.1
Cation exchange capacity (CEC)	12.0 mequiv./100g

ter contents ranging from 15.5 to 23% and densities ranging between 1.562 and 1.747 Mg/m³. The higher water contents obtained at the upper part of the clay liner may be attributed

Fig. 1. Photograph of a typical crack located at the edge of a seam.



to the trapped water observed between the geomembrane and the compacted clay along with negligible effective stress at and near the clay surface that may have caused the clay to swell at the surface and hence increase the water content. This may also be partially due to the increase in void ratio from the biological activity that has taken place at and near the interface (in the form of the aforementioned black sludge) similar to the observations reported by Hrapovic

(2001) for laboratory tests on clay plugs under negligible effective stresses.

Properties of the geomembrane after 14 years

Geomembrane samples were taken from the anchor trench (NSNL: no sunlight exposure, no leachate exposure), above

the leachate levels in the lagoon (SNL: sunlight but no leachate exposure), at the leachate level interface (SLI: sunlight and leachate exposure), and below the leachate level (NSL: no sunlight but leachate exposure). Selected samples were also taken from the bottom of the lagoon (NSLB: no sunlight but leachate and significant sludge exposure). Figure 2 schematically shows the different locations from which the samples were collected.

ASTM methods

The following ASTM methods were used to evaluate the samples:

ASTM D 883	Standard definitions of terms relating to plastics, Vol. 08.01
ASTM D1004	Standard test method for initial tear resistance of plastic film and sheeting, Vol. 08.01
ASTM D1238	Flow rates of thermoplastics by extrusion plastometer, Vol. 08.01
ASTM D1603	Standard test method for carbon black in olefin plastics, Vol. 08.01
ASTM D3350	Standard specification for polyethylene plastics pipe and fittings materials, Vol. 08.02
ASTM D3895	Standard test method for oxidative-induction time of polyolefins by differential scanning calorimetry, Vol. 08.02
ASTM D4437	Standard practice for determining the integrity of field seams used in joining flexible polymeric sheet geomembranes, Vol. 04.09
ASTM D5397	Standard test method for evaluation of stress crack resistance of polyolefin geomembranes using notched constant tensile load test, Vol. 04.09
ASTM D5885	Standard test method for oxidative induction time of polyolefin geosynthetics by high-pressure differential scanning calorimetry, Vol. 04.09
ASTM D638–90	Standard test method for tensile properties of plastics, Vol. 08.01
ASTM D792	Standard test methods for density and specific gravity (relative density) of plastics by displacement, Vol. 08.01
ASTM E794	Standard test method for melting and crystallization temperatures by thermal analysis, Vol. 14.02

Geomembrane sheet samples

Oxidative induction time (OIT)

The first step of HDPE oxidative degradation is the consumption of the antioxidant used to hinder oxidation of the geomembrane. The amount of the antioxidant in the geomembrane is usually evaluated in terms of the oxidative induction time (OIT) using either the standard (Std) OIT test (ASTM D3895: 200°C, 35 kPa) or the high pressure (HP) OIT test (ASTM D5885: 150°C, 3500 kPa). A discussion of these two test methods has been presented by Hsuan and Koerner (1998).

The OIT values for modern HDPE geomembranes are typically in the range of 100 or more minutes. As shown in Ta-

ble 4, average OIT (standard) values for all exposure conditions were very low implying that there were only small amounts of antioxidant in the geomembrane at the time of sampling. Of all the sampling locations, those denoted "SNL" were exposed to the greatest amounts of sunlight, the highest temperatures, and the most abundant amounts of oxygen. Thus these samples might be expected to have experienced the greatest photo-oxidation (UV) and thermo-oxidation (temperature), and indeed the average OIT of 1.8 min (based on 12 tests) was well below that of the other exposure conditions (see Table 4). The OIT of 1.8 min is close to the OIT value of 0.5 min measured by Hsuan and Koerner (1998) for an unstabilized (without any antioxidant) HDPE geomembrane, and the possibility that degradation might already have started in the exposed geomembrane cannot be excluded.

The OIT values were slightly higher (5–6 min) for samples below the leachate level (NSLS and NSLB) than for SNL samples, suggesting that more antioxidant remained in these samples. Factors that can affect antioxidant consumption include temperature and the availability of oxygen (Hsuan and Koerner 1998; Sangam 2001). The samples below the leachate level would experience the most consistent temperature and the lowest maximum temperature in the entire liner system. The leachate temperature would remain relatively constant throughout the year unlike the surface temperature, which would vary significantly. Secondly, oxygen would not be as abundant in the leachate as in the air even though the lagoon was aerated.

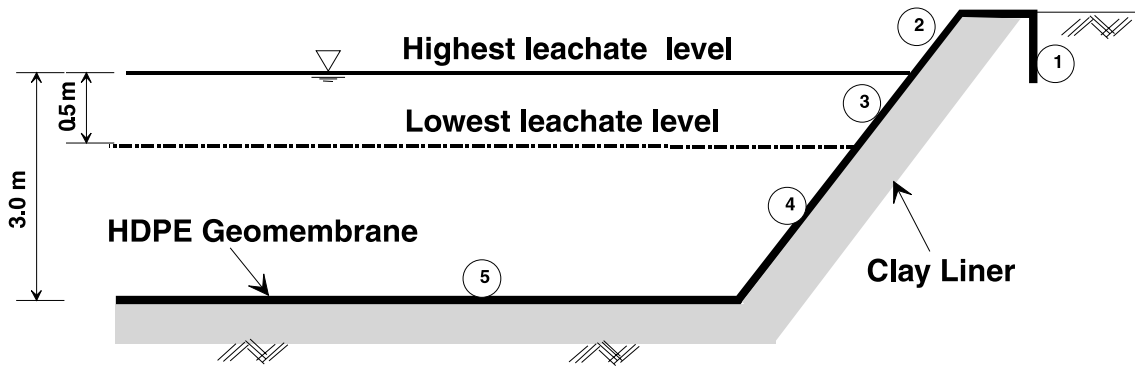
The SLI samples that had been subjected to intermittent sunlight and leachate exposure had an average OIT of 3 min, which was intermediate between the values obtained for full sun and full leachate exposure. A similar value was obtained for the anchor trench sample (NSNL) that was obtained from a shallow depth (approximately 0.75 m). At this depth, the temperature would reach 28°C during the summer and, as a consequence, the degradation would be expected to be faster than for samples covered by leachate.

Since the initial OIT of the original material at the time of installation was not available, it was rather difficult to infer the exact rate at which the antioxidant had been depleted. However, Adams and Wagner (2000) indicated that in the 1980s (i.e., the period when the geomembrane being discussed was manufactured and installed), the OIT of HDPE geomembranes was typically around 50 min (not the typical value of 100 min or more for modern geomembranes). Using that value as a basis and assuming that the depletion of antioxidants follows the first order decay kinetics as shown by Hsuan and Koerner (1995, 1998) and Sangam (2001), it can be estimated that the depletion of these specific antioxidants present in the geomembrane proceeded at approximately 0.24 year⁻¹ for the exposed samples and at about 0.15 year⁻¹ for samples covered by the leachate. The depletion rate for exposed samples compared very well with the rate of 0.28 year⁻¹ based on data provided by Hsuan et al. (1991).

Density, carbon black content, and crystallinity

Since HDPE is a semicrystalline material, its density may be related to its degree of crystallinity. The density of five specimens cut from each sample was obtained according to ASTM D792, and the average values are presented in Ta-

Fig. 2. Localization of geomembrane samples (not to scale).



Not to scale

- | | | |
|--------------------------------|------|------------------------------------|
| 1. Anchor trench | NSNL | (No sunlight, no leachate) |
| 2. Above leachate level | SNL | (Sunlight, no leachate) |
| 3. Leachate level interface | SLI | (Sunlight and leachate) |
| 4. Below leachate level-slope | NLSL | (No sunlight, leachate) |
| 5. Below leachate level-bottom | NSLB | (No sunlight, leachate and sludge) |

Table 4. Summary of the physical, chemical, and mechanical properties (modified from Rowe et al. 1998) of the samples according to various ASTM methods.

Sample	D3895 Sdt-OIT (min)	D1603 CBC (%)	D792 ρ_g (g/cm ³)	E794 χ (%)	D5397 SCR (h)	D1238 MFI (g/10 min)	D638				D1004 ITR (N)
							Tensile yield		Tensile break		
							<i>T</i> (kN/m)	ϵ (%)	<i>T</i> (kN/m)	ϵ (%)	
NSNL	3.5	2.58	0.965	—	3.5	0.36	37	11	33	646	283
SNL	1.8	2.64	0.967	67.5	2.6	0.50	37	11	25	379	274
SLI	3.3	2.67	0.967	—	—	—	37	10	26	479	284
NLSL	6.3	2.73	0.966	65.7	3.1	0.41	37	11	32	703	282
NSLB	5.0	2.20	0.965	65.5	3.0	0.31	39	10	27	456	292

Note: The results represent the average of replicate tests for the area considered. Sdt-OIT, standard oxidative induction time; CBC, carbon black content; ρ_g , density; χ , crystallinity; SCR, stress crack resistance; MFI, melt flow index; *T*, strength; ϵ , strain; ITR, initial tear resistance.

ble 4. The results are very similar for all locations and vary slightly between 0.965 and 0.967 g/cm³.

The measured densities include a contribution due to the carbon black content (CBC), which can increase the overall density of the geomembrane by 0.0044 for each 1% of carbon added (ASTM D3350). Back-calculating to estimate the effect of CBC gave estimated resin densities of about 0.954–0.955 g/cm³. These values were higher than those suggested as typical values for copolymer HDPE (0.941–0.950 g/cm³) and suggest a high degree of crystallinity and hence a stiffer and more brittle geomembrane than modern copolymer HDPE geomembranes. Thus, it may be expected that the geomembrane will have higher tensile strength and lower strains at yield and break and will be more susceptible to stress cracking than modern HDPE geomembranes. This likely reflects the manufacturing practice of the time and may not be necessarily attributable to ageing.

The crystallinity, as evaluated according to ASTM E794 using a differential scanning calorimeter (DSC), ranged from 65 to 67% (see Table 4). These results are indicative of a

very high degree of crystallinity and are consistent with the high densities measured. One of the expected consequences of high crystallinity would be an increased susceptibility of the geomembrane to stress cracking. If this is the case, then the SNL samples with the highest crystallinity would be expected to have the lowest stress cracking resistance.

Tensile and tear characteristics

The tensile properties, obtained according to ASTM D638–90 (Type IV) and summarized in Table 4, show no significant difference with sample location in either strength or strain values at yield. The yield strength (37–39 kN/m) was higher than for typical modern geomembranes (30 kN/m), while the strains at yield (10–11%) were lower than for typical modern geomembranes (15%), implying a stiffer material than would be expected for a modern material.

Both the strength and strain values at break were lower than those expected for new modern material. The highest values of 33 and 32 kN/m were obtained for the anchor

trench samples (NSNL) and the samples from the slope that were exposed to leachate (NSLS), respectively. The lowest values of 25 and 26 kN/m were measured for samples exposed to sun (SNL) and samples from the leachate–sunlight interface (SLI), respectively. However, a surprising low value of about 27 kN/m was also obtained at the bottom (NSLB). It is hypothesized that this low value is due to the scratched nature of bottom samples, probably induced by the maintenance activities of the lagoon. These results are consistent with those reported by Rollin et al. (1994) who observed, for a 7-year-old HDPE, an increase of strength at yield and a decrease of both strength and strain at rupture. This behaviour of HDPE geomembranes suggests that the material has become brittle, and it would be consistent with ageing of the geomembrane.

The initial tear resistance (ITR) of a geomembrane (ASTM D1004) is defined as the load required to initiate tearing of the material. The values obtained for samples from different locations (see Table 4) suggest that the sun exposed (SNL) samples had the lowest ITR and those from the bottom of the lagoon had the highest. This contrasts with the low break strength measured for the sample collected from the bottom of the lagoon that had been scratched. This is attributed to the fact that in the ITR test, samples are notched and therefore are less influenced by surface defects.

Melt flow index

The molecular weight of the HDPE is related to the melt flow index (MFI) of the polymer with a low MFI corresponding to longer average polymer chains. The MFI values obtained (ASTM D1238) from different locations (Table 4) ranged between 0.31 and 0.50 g/10 min, with the lowest value corresponding to samples fully covered by leachate (NSLS and NSLB), whereas the exposed samples (SNL) had the highest value of 0.50 g/10 min. This, like other evidence discussed earlier, is consistent with the most exposed (SNL) samples having experienced the greatest degradation (giving rise to the smallest molecular chains) and those near the bottom of the lagoon the least degradation. The findings are in stark contrast to the observations made by Hsuan et al. (1991) for a 7-year-old HDPE geomembrane where the lowest MFI was measured for exposed samples.

Stress cracking resistance (SCR)

Stress cracking has been defined (ASTM D883) as an external or internal rupture in a plastic caused by a tensile stress less than its short-term mechanical strength. In the present investigation, the SCR was assessed by the single notched constant load test (SP-NCLT) following the procedure described in ASTM D5397. The notch was introduced from the exposed side of the geomembrane to minimize surface effects such as scratches or any surface degradation.

The SCR, reflected by the failure time given in Table 4, is remarkably low with all specimens failing within 4 h compared to the 200 h specified for a new modern HDPE geomembrane (Hsuan and Koerner 1997). Since the SCR data for the original geomembrane was not available, one cannot assess whether or not the low cracking resistance is due to ageing. Nevertheless, it is apparent that the exposed geomembrane had a lower failure time (i.e., more susceptible to stress cracking) than that of the covered samples. This

is consistent with other properties measured (MFI, tensile and initial tear resistance) suggesting that the exposed samples have experienced more degradation than samples from other locations.

Seams

Shear and peel tests (ASTM D4437) were used to evaluate the quality and the integrity of the seams. In general, as quality control criteria, it is recommended that the ratio between the shear strength of the seam and the tensile strength of the sheet at yield be greater than 90%, while the peel strength should be greater than 75% of the sheet strength at yield. Also, the seam strain at break must not be less than that of the sheet (ratio greater than 100%). The results of the shear and peel tests performed on five test specimens cut from seam samples collected from four different locations (SNL, SLI, NSLS, and NSLB) are summarized in Table 5.

Except for the NSLB sample, the shear strength ratios are below today's typical quality control criteria with values less than 70%. The peel test results presented showed very low seam-sheet strength ratios (<30%) compared to today's typical quality control criterion of 75%, suggesting either very poor initial welding or a significant loss of peel strength during the 14 years of exposure.

Contaminant diffusion through the geomembrane

Materials and methods

Sorption and diffusion tests were conducted on samples from locations SNL, NSLS, and NSLB (see Fig. 2). The tests examined seven organic chemicals (Table 6) representative of chlorinated hydrocarbons (dichloromethane (DCM); 1,2-dichloroethane (1,2-DCA); and trichloroethylene (TCE)) and aromatic hydrocarbons (benzene, toluene, ethylbenzene, and xylenes (BTEX)).

The tests were performed at room temperature ($22 \pm 2^\circ\text{C}$) using mixed dilute aqueous solutions with the concentration of each contaminant at about 5 mg/L. Solution samples collected from the cells during the test were analyzed using a Varian gas chromatography – mass spectrometer (GC/MS) consisting of a Saturn 2000 MS and a 3800 GC equipped with a 8200 CX autosampler used in solid phase micro-extraction (SPME) and headspace modes. The contaminant concentrations were quantified based on calibration curves obtained through analysis of standards of known concentrations that were regularly prepared during the tests. Details regarding the test and the analytical procedure used are given in Sangam and Rowe (2001).

In the sorption tests, geomembrane samples were immersed in glass cells filled with a mixed dilute solution of contaminants. The change in contaminant concentration in the solution was monitored with time until equilibrium was reached, and then the partitioning coefficients (S_{gr}) were deduced as described by Sangam and Rowe (2001).

The diffusion tests were performed in double glass compartment cells consisting of a closed system with source and receptor reservoirs separated by the geomembrane sample under investigation as described by Rowe (1998) and Sangam and Rowe (2001). During the test, concentrations in both source (a mixed aqueous solution with each contami-

Table 5. Shear and peel test results on seams collected from different locations (ASTM D4437).

Test	Sample	Yield				Break				Type of failure*
		Strength		Strain		Strength		Strain		
		<i>T</i> (kN/m)	% Sheet	ε (%)	% Sheet	<i>T</i> (kN/m)	% Sheet	ε (%)	% Sheet	
Shear	SNL	24	65	6	55	24	73	7	2.1	1a, 3b, 1c
	SLI	20	54	3	27	20	80	3	0.6	5b
	NLSL	25	66	4	36	25	96	5	0.7	1a, 4b
	NSLB	36	92	7	70	35	130	9	2	4b, 1d
	SNL					6	16	65	17	1a, 4b
Peel	SLI					5	14	10	2	1a, 4b
	NLSL					4	11	70	10	5b
	NSLB					10	20	178	39	1a, 3b, 1d

Note: Values are the average of 10 samples tested.

*The number denotes the number of failures and the letter denotes the type of failure where: a is a failure in adhesion; b is a break through the fillet; c is a break at the seam edge (bottom sheet); and d is a break in the bottom sheet.

Table 6. The properties (from Montgomery and Welkom 1990) of organic contaminants and the range of partitioning coefficients, S_{gf} , deduced from sorption tests.

Chemicals	Formula	Molar weight (g/mole)	Density (g/cm ³)	Molar volume* (cm ³)	Aqueous solubility† (mg/L)	Octanol–water (log K_{ow})	Dipole moment (Debye)	Partitioning coefficient S_{gf} (–)
Chlorinated hydrocarbons								
Dichloromethane	CH ₂ Cl ₂	84.93	1.3266	64.02	20 000	1.25	1.60	3–5
1,2-Dichloroethane	C ₂ H ₄ Cl ₂	98.96	1.2530	78.98	8 690	1.45	1.44	6–8
Trichloroethylene	C ₂ HCl ₃	131.39	1.4642	89.74	1 100	2.53	0.77	53–56
Aromatic hydrocarbons								
Benzene	C ₆ H ₆	78.11	0.8765	89.11	1 780	2.13	0.00	20–24
Toluene	C ₇ H ₈	92.14	0.8669	106.28	515	2.79	0.30	57–69
Ethylbenzene	C ₈ H ₁₀	106.17	0.8670	122.46	152	3.13	0.36	130–156
<i>m</i> -Xylene	C ₈ H ₁₀	106.17	0.8642	122.85	162	3.20	0.30	190–216
<i>o</i> -Xylene	C ₈ H ₁₀	106.17	0.8802	120.62	152	3.13	0.63	170–180
<i>p</i> -Xylene	C ₈ H ₁₀	106.17	0.8669	122.47	156	3.18	0.00	190–216

*Calculated based on chemical density and molar weight.

†At 20°C.

nant listed in Table 6 at 5 mg/L) and receptor (initially deionized distillate water) reservoirs were monitored with time and the results were plotted as normalized concentrations (i.e., the concentration at a given time divided by the initial source concentration), as shown in Figs. 3 and 4.

The governing differential equation in these diffusion tests can be expressed as

$$[1] \quad \frac{\partial c_g}{\partial t} = D_g \frac{\partial^2 c_g}{\partial z^2}$$

where D_g is the diffusion coefficient of the geomembrane [L^2T^{-1}], c_g is the concentration of diffusing substance in the geomembrane [ML^{-3}], and z is the direction of diffusion [L]. Since the concentrations (c_f) in the reservoir are monitored, then the flux, f [$ML^{-2}T^{-1}$], associated with the process can be written as (Rowe 1998; Sangam and Rowe 2001)

$$[2] \quad f = -S_{gf} D_g \frac{dc_f}{dz} = -P_g \frac{dc_f}{dz}$$

where P_g [L^2T^{-1}], referred to as the permeation coefficient, is a contaminant mass transfer coefficient and S_{gf} [–] is the partitioning coefficient of the contaminant between the geomembrane and the adjacent fluid and is dependent upon the chemical–geomembrane system.

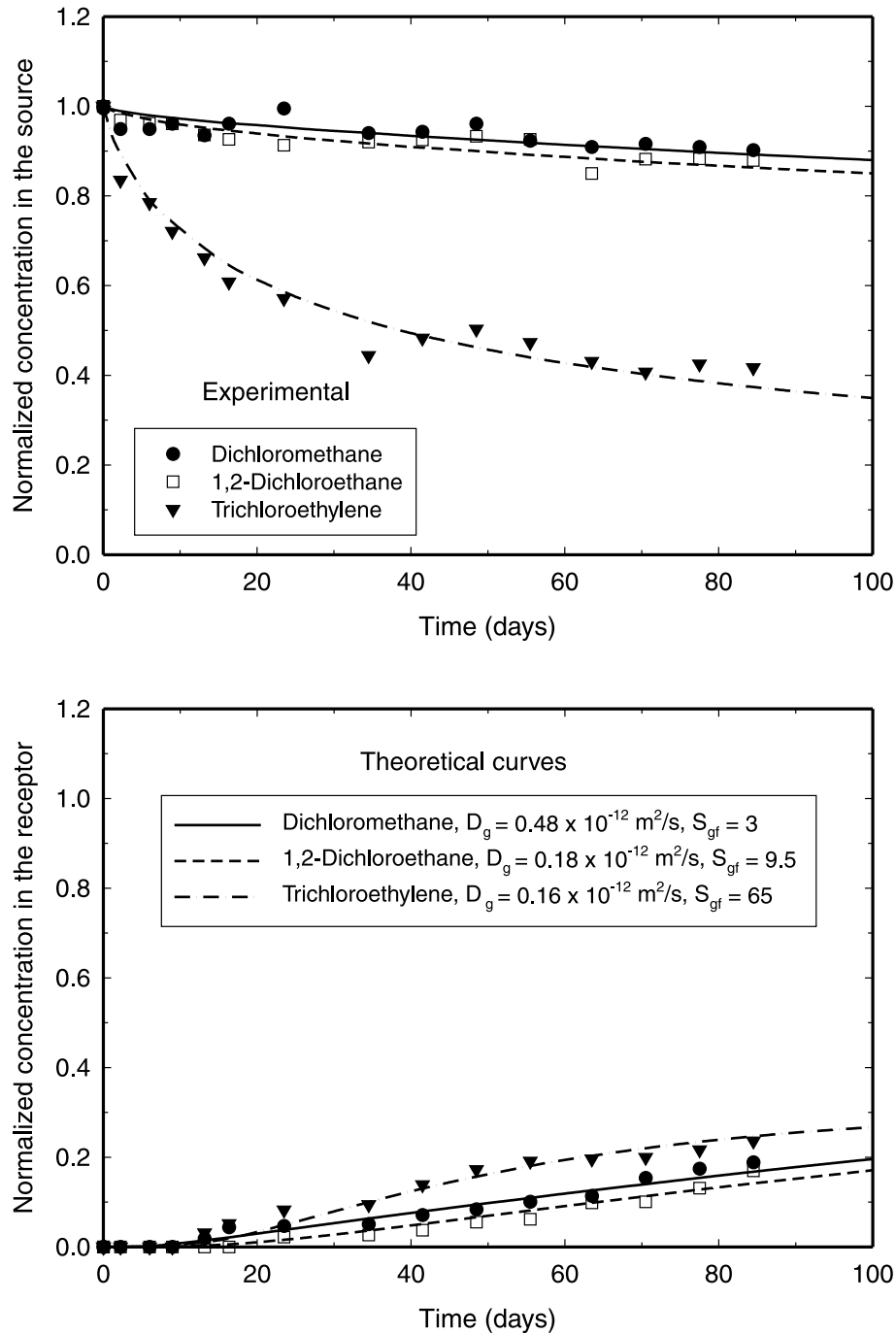
The tests were analyzed following the procedure described in detail by Rowe et al. (1995a) using the finite layer analysis program POLLUTE[®] v6.3.6 (Rowe et al. 1999) that specifically allows the modelling of the phase change and the boundary conditions in these tests.

Test results

Sorption test

Partitioning coefficients calculated based on the sorption tests are summarized in Table 6 (full test data is given by Sangam 2001). For the chlorinated aliphatic compounds examined, TCE has the highest value of S_{gf} (53–56), followed by DCA with a S_{gf} of 5–8. The lowest S_{gf} (3–5) was measured for DCM. For aromatic compounds, the calculated S_{gf} is the highest for *m*- and *p*-xylenes with values between 190

Fig. 3. Variation in the chlorinated hydrocarbons in the source and receptor during diffusion tests for sample SNL.

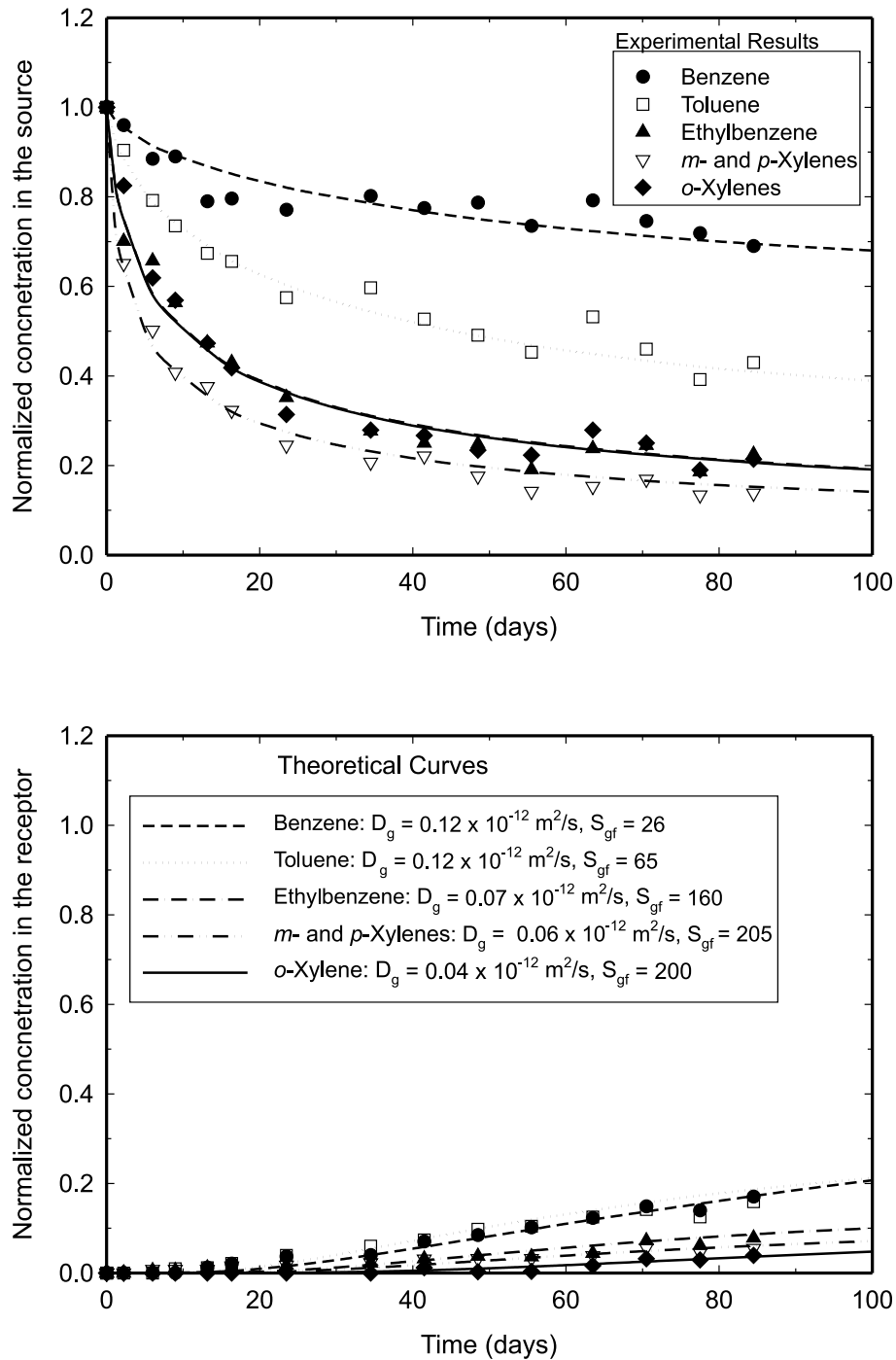


and 216, while benzene has the lowest S_{gf} at about 20–24. Although there was some (relatively small) variability in the results for a given compound, there was no significant or consistent difference among the results from the different sample locations. This may be attributed to the fact that the crystallinity of the samples was similar at the three locations (with the average ranging from 65.5 to 67.5%).

Diffusion test

Contaminant concentrations (measured in the source and

the receptor over the 85 days of testing for the SNL sample) obtained for chlorinated hydrocarbons and aromatic hydrocarbons are shown in Figs. 3 and 4, respectively. In these plots, data points represent the average of triplicate values quantified with GC analyses. As previously discussed by Sangam and Rowe (2001), in this type of test the decrease in the source concentration is controlled by the partitioning parameter (S_{gf}) while the increase in the receptor concentration is dominated by the permeation coefficient (P_g). The diffusion curves were very similar for samples from all locations

Fig. 4. Variation in the aromatic hydrocarbons in the source and receptor during diffusion tests for sample SNL.

(SNL, NSLS, and NSLB). Full data for all samples is provided by Sangam (2001).

Of the chlorinated compounds, the greatest (60%) decrease in the source solution concentration was for TCE (see Fig. 3), which dropped to 40% of the initial concentration after 85 days of testing. In contrast, the source concentrations of DCM and 1,2-DCA decreased by less than 10% over 85 days. In all cases, there was significant mass transfer to the receptor reservoir with the greatest increase being for TCE and the smallest for 1,2-DCA. The fact that the source

concentration for 1,2-DCA decreased more than for DCM but the receptor increased less provides qualitative information about the sorption and diffusion coefficients, implying higher sorption and lower diffusion for 1,2-DCA than for DCM since there is greater uptake of 1,2-DCA by the geomembrane but less mass transfer through the geomembrane and into the receptor.

Figure 4 shows the variation in the concentration of aromatic hydrocarbons for the SNL sample during the diffusion test period. From the source data, it can be seen that after

85 days of testing, the benzene concentration decreased by about 30% while that of toluene, *o*-xylene, and the *m*- and *p*-xylenes dropped by about 50, 80, and 85%, respectively. The increase in concentration in the receptor was greatest for benzene and toluene followed by ethylbenzene, the *m*- and *p*-xylenes, and *o*-xylene.

The theoretical curves generated for each of the compounds by solving the governing differential equation subject to the appropriate boundary conditions are also shown as lines in Figs. 3 and 4. By obtaining the best fit to the source and the receptor concentrations one can deduce the values of S_{gf} and D_g and hence calculated P_g as summarized in Table 7.

Discussion

The S_{gf} values (see Tables 6 and 7) generally increase with an increase in the *n*-octanol–water coefficient ($\log K_{ow}$) (which indicates the chemical hydrophobicity, and hence the ability of the chemical to partition with organic material). The partitioning coefficient varied somewhat from sample to sample in both the sorption (Table 6) and diffusion (Table 7) tests, however, the magnitude of the partitioning was very similar for both of the tests.

Comparing the diffusion test results obtained for samples from three different locations (see Table 7), it can be seen that while there is some small variability there is no consistent trend that could be attributed to location or to the small difference in crystallinity, and the range of values considered is more an indication of the variability that can be obtained among different samples of similar material in this type of test.

It is of some interest to compare the diffusion and sorption characteristics of the 14-year-old geomembrane (Table 7) with those obtained by Sangam and Rowe (2001) for an unaged modern HDPE geomembrane (see Table 8). The primary relevant difference between the two geomembranes is the crystallinity (65–68% and 47% for the old and new geomembranes, respectively). As is evident from Table 8, the permeation coefficient, P_g , is substantially higher for the new geomembrane than for the old one (by a factor of between 1.7 and 4.8). In fact, the difference in permeation coefficient between the two geomembranes is compound specific with the smallest difference being for DCM (which has the lowest molecular volume), and it generally increases with increasing molar volume. Benzene and TCE have a similar molar volume and a similar difference in permeation coefficients between old and new geomembranes. The greatest difference was for ethylbenzene and xylenes, which all have a similar molar volume (120.6–122.8 cm³). This observed reduction in permeation coefficient may be attributed to the high crystallinity of the samples. As indicated by Naylor (1989) and Rogers (1985), the crystalline zones in semicrystalline polymers act as relatively impermeable barriers to the migrating molecules by (1) reducing the sorptive and diffusive regions, and (2) restraining the mobility of the polymer molecules required for the accomplishment of the diffusive jump. As a consequence, the segmental mobility of the chains required to achieve migration are restrained, and therefore the diffusion process becomes more dependent on the size and shape of the migrating molecule (Naylor 1989; Rogers 1985).

Effectiveness of the geomembrane liner

It is well recognized that an intact HDPE geomembrane is an excellent barrier to advective migration as well as an excellent diffusive barrier against inorganic and polar contaminants. Chloride is an inorganic ion that has a very low diffusion coefficient through HDPE geomembranes (Rowe et al. 1995a). Theoretically, if the HDPE geomembrane examined in this study stayed relatively intact for any length of time, very little break-through of chloride would be observed in the compacted clay liner. Conversely, if significant amounts of chloride (above background levels) were to be present in the compacted clay, this would suggest that the geomembrane had failed to perform its intended task.

Figure 5 shows the chloride concentration profile through the clay liner at the time of the investigation (i.e., after 14 years of service) measured from squeezed pore fluid obtained from five boreholes drilled into the clay liner. The profile shows an apparent back diffusion near the top, probably due to dilution of the leachate present in the bottom of the lagoon (rainwater that had accumulated during the one month period between decommissioning and the investigation). After 14 years of service, chloride had migrated approximately 1.7 m, which is consistent with expectations based on previous field cases in which the leachate was in direct contact with the clay liner (e.g., Rowe et al. 1995b). Although the clay liner appeared to have performed well (there was over 1.0 m of clay below the contaminated zone with no chloride) in protecting the environment during the service period, there are still questions about the effectiveness of this particular geomembrane liner in impeding the migration of chloride.

The effectiveness of the geomembrane with respect to contaminant migration was evaluated via contaminant transport modelling (using POLLUTE[®] v6.3.6, Rowe et al. 1999). Chloride leachate concentrations as shown in Fig. 6 were used to predict chloride pore-fluid concentrations throughout the compacted clay based on different assumptions regarding when the geomembrane failed. These profiles were then compared to chloride pore-fluid concentrations obtained from the field investigation.

For modelling purposes, the clay liner was subdivided into three layers (0–0.25, 0.25–0.50, and >0.50 m) with porosities of 0.48, 0.42, and 0.38, respectively, to account for the variation in water content with depth. The average value of the clay hydraulic conductivity (measured using flexible wall hydraulic conductivity tests with an effective stress ranging from 30 to 50 kPa and a gradient across the sample of 20) was about 2.2×10^{-10} m/s. The chloride diffusion coefficient for the clay measured in the laboratory was about 7×10^{-10} m²/s.

Prediction of chloride pore-fluid profiles through the compacted clay requires consideration of the effectiveness of the geomembrane during the lifespan of the lagoon. If the geomembrane was intact (no defects), then chloride pore-fluid concentrations through the clay should be close to background levels because of the very low diffusion of chloride through geomembranes (Rowe 1998). For initial comparison purposes, it is interesting to examine the theoretical chloride contaminant profile through the clay for the unlikely scenario that the geomembrane was intact with only 2.5 holes

Table 7. Inferred partitioning and diffusion coefficients based on diffusion tests with aqueous solutions.

Chemicals	Sample SNL ($\chi = 67.5\%$)			Sample NSLS ($\chi = 65.7\%$)			Sample NSLB ($\chi = 65.5\%$)		
	S_{gf} (-)	D_g (10^{-12} m ² /s)	P_g (10^{-12} m ² /s)	S_{gf} (-)	D_g (10^{-12} m ² /s)	P_g (10^{-12} m ² /s)	S_{gf} (-)	D_g (10^{-12} m ² /s)	P_g (10^{-12} m ² /s)
Chlorinated hydrocarbons									
Dichloromethane	3	0.48	1.4	3	0.5	1.5	5	0.45	2.3
1,2-Dichloroethane	10	0.18	1.8	10	0.16	1.6	10	0.16	1.6
Trichloroethylene	65	0.16	10.4	60	0.18	10.8	68	0.17	11.6
Aromatic hydrocarbons									
Benzene	26	0.12	3.1	32	0.12	3.8	32	0.13	4.2
Toluene	65	0.12	7.8	70	0.14	9.8	70	0.15	10.5
Ethylbenzene	160	0.07	11.2	160	0.08	14.4	150	0.08	12.0
<i>m</i> - and <i>p</i> -Xylenes	205	0.06	12.3	220	0.08	17.6	205	0.08	16.4
<i>o</i> -Xylene	200	0.04	8.0	190	0.06	11.4	180	0.06	13.3

Note: χ , crystallinity.

Table 8. Comparison of calculated permeation coefficients for the 14-year-old geomembrane (old GM) and the new modern geomembrane (new GM).

Chemicals	New GM* ($\chi = 47\%$)			Old GM ($\chi = 65.5-67.5\%$)	
	S_{gf}	D_g (10^{-12} m ² /s)	P_g (10^{-12} m ² /s)	P_g (10^{-12} m ² /s)	$\left[\frac{P_g \text{ (new GM)}}{P_g \text{ (old GM)}} \right]$ (-)
Chlorinated hydrocarbons					
Dichloromethane	6	0.65	3.9	1.4-2.3	1.7-2.8
1,2-Dichloroethane	12	0.40	4.8	1.6-1.8	2.7-3.0
Trichloroethylene	85	0.40	34.0	9.6-11.6	1.9-3.5
Aromatic hydrocarbons					
Benzene	30	0.35	10.5	3.1-4.2	2.5-3.4
Toluene	100	0.30	30.0	7.8-10.8	2.9-3.8
Ethylbenzene	285	0.18	51.3	9.8-12.0	3.6-4.6
<i>m</i> - and <i>p</i> -Xylene	347	0.17	59.0	12.3-17.6	3.4-4.8
<i>o</i> -Xylene	260	0.15	36.0	8.0-13.3	3.2-4.5

Note: χ , crystallinity.

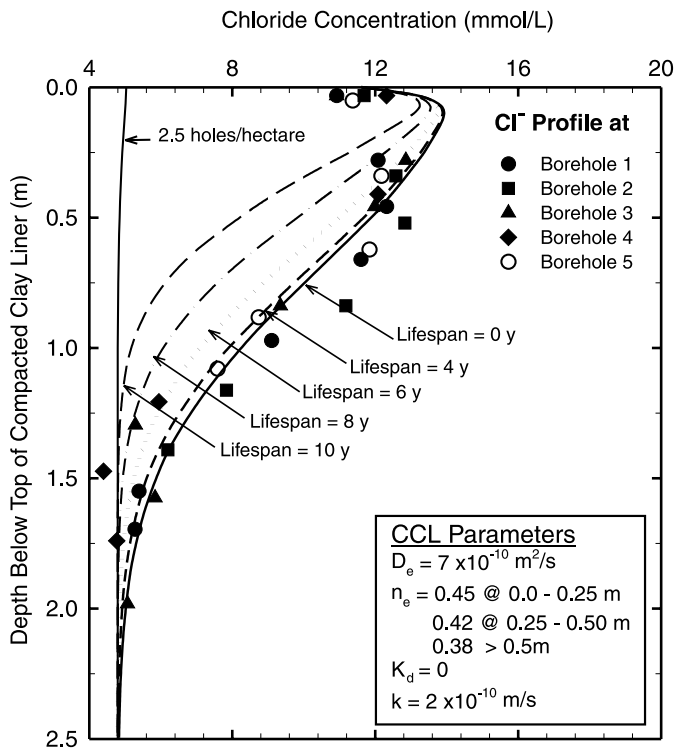
*From Sangam and Rowe (2001).

(5 mm diameter) per hectare throughout the entire lifetime of the lagoon. It should be noted again that approximately 528 defects per hectare were actually found on the geomembrane at the time of the investigation. Based on the given leachate concentrations (Fig. 6) and a Darcy velocity (flux) of 3.5×10^{-4} m/a (1.1×10^{-11} m/s) through the geomembrane and clay, the resultant chloride profile through the clay is shown in Fig. 5. Leakage through the geomembrane was calculated with the LEAK program (Rowe and Lake 1997) using similar parameters to those summarized by Rowe (1998). As can be seen from Fig. 5, theoretical chloride concentrations are severely underpredicted through the compacted clay liner, and there is no match to the contaminant profiles obtained from the field investigation. This is because chloride leakage through a few small holes combined with a low chloride diffusion coefficient through the geomembrane gives rise to very little chloride flux through the geomembrane liner.

As a result of observations made during the field investigation, as well as discussions with maintenance staff, it is

apparent that modelling of the composite liner by assuming leakage through only a few holes in the geomembrane is not very realistic. A significant amount of leachate was observed to be trapped under the geomembrane and was in direct contact with the compacted clay. It may be inferred that at some point during the lifetime of the lagoon, the geomembrane stopped functioning as an effective barrier and started to allow significant contact between the leachate and the compacted clay. Figure 5 shows contaminant profiles for chloride assuming the geomembrane was ineffective from the time of construction (lifespan equals 0 years) as well as various times after construction (4, 6, 8, and 10 years). In other words, after these time periods, modelling assumed that the leachate was in direct contact with the compacted clay and that the geomembrane had no influence on leachate contact with the clay. A comparison of the theoretical curves with the field data suggests that the geomembrane was effective for less than 8 years of the 14-year lifespan of the lagoon. Theoretical chloride pore-fluid profiles assuming geomembrane failure at 8 and 10 years provide a poor fit to

Fig. 5. Chloride concentration profile through the compacted clay liner based on samples from five boreholes together with prediction of pore-fluid concentration for different assumed geomembrane service lives.



experimental chloride pore-fluid concentrations. However, assuming the geomembrane functioned effectively for elapsed times of 0, 4, and 6 years after construction provides a reasonable fit to the majority of the data.

Based on this chloride modelling, it is considered likely that the geomembrane ceased functioning effectively somewhere between 0 and 4 years after construction. However, there is some scatter in the field chloride pore-fluid concentrations that causes some uncertainty as to the actual time of failure of the geomembrane. It is also unlikely that the geomembrane failed at the same time for the entire lagoon, and hence the sequence by which the failure occurred would be expected to have some effect on the field profiles at different locations. Figure 5 contains data from five different locations and some scatter in field chloride concentration profiles is likely due to this effect. However, the general conclusion that the geomembrane failed to function effectively at some time 0–4 years after construction is consistent with discussions with the operators of the landfill, who indicated that frequent maintenance of the geomembrane was required almost from the time of installation.

Composite liner design implications

As previously mentioned, the level of understanding of using geomembranes with compacted clay for lagoons and landfills has improved considerably as results of case histories are published and discussed. The findings of this partic-

ular study reinforce existing design philosophies as well as the need for proper construction quality control and material selection. Below is a discussion of these items.

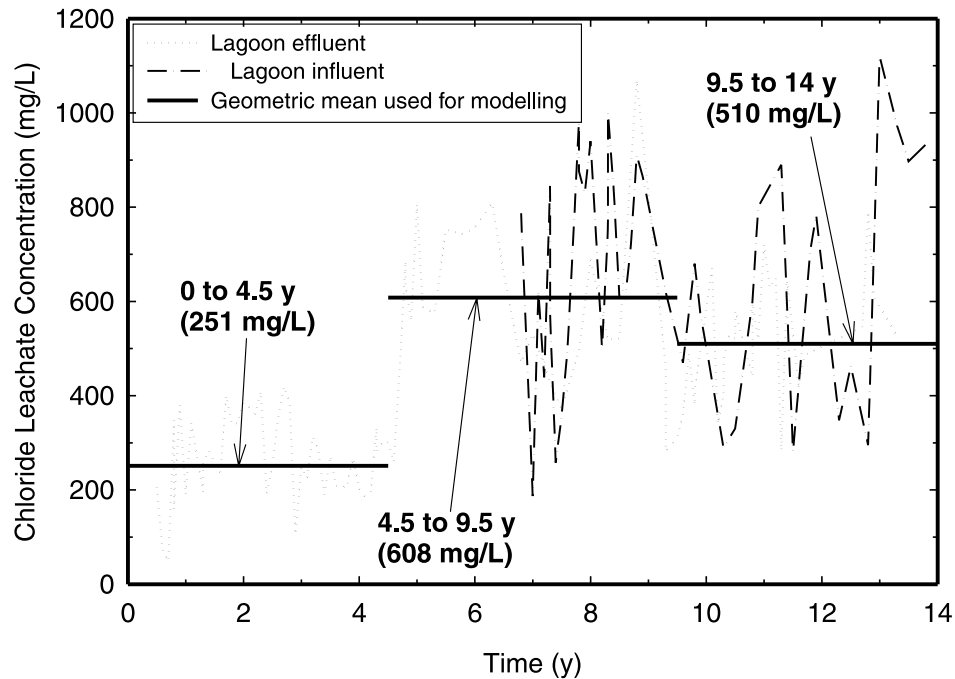
(1) The vintage of the geomembrane component of the lagoon liner discussed in this paper most likely did not fall within the time period where proper construction quality control was practiced for small lagoons such as this one. However, it is believed that observations of poor seam quality and geomembrane wrinkles were the result of construction practices. This reinforces the need for experienced installation personnel as well as qualified construction control – assurance procedures.

(2) The geomembrane material properties exhibited undesirable values with respect to OIT, CBC, crystallinity, and SCR. Because of a lack of knowledge of the original geomembrane properties, it is unknown whether this is the result of degradation or simply different geomembrane properties compared to similar products of that vintage. However, it does highlight the importance of proper geomembrane specifications (i.e., OIT, crystallinity, and SCR). Typical values for Std-OIT of 100 min, for CBC of 2–3%, for crystallinity of 45–50%, and for SCR of 200 h, as proposed by Hsuan and Koerner (1997) and Hsuan (2000), should be a minimum for lagoon liners such as this one.

(3) It is believed that some of the defects observed in the liner were the result of maintenance activities. Material selection, such as a thicker geomembrane (e.g., 2.0 mm), may have helped with durability but may have made it more difficult to construct for the small geometry. Also, protection of the geomembrane with a thick geotextile and (or) sand layer would help during maintenance activities as well as providing protection from sunlight. Stability issues would have to be addressed as part of this process (Koerner 1999). Narejo et al. (1996), Koerner (1999), and Tognon et al. (2000) provide some insight regarding the design of protection layers. Maintenance of the lagoon should be part of the design and planning stage. Special care should be taken during sludge removal, and travel areas should be given additional protection for trucks and maintenance workers. Such care can help minimize maintenance-induced defects on the liner.

(4) Designing a lagoon for contaminant transport involves selection of the proper diffusion coefficient. The results obtained herein, along with those reported by Sangam (2001), suggest that volatile organic compound (VOC) diffusion coefficients will decrease with increasing crystallinity of the geomembrane. If the crystallinity does increase with geomembrane ageing as reported by several investigators (e.g., Sangam 2001), then it is conservative to use the diffusion coefficients of the unaged material. However, as shown in this paper, if diffusion coefficients decrease substantially with the increase of the crystalline zone in the geomembrane, other defects such as cracks, holes, and tears may result causing advective flow through these defects to control the overall contaminant transport through the geomembrane portion of the composite liner system.

(5) The importance of the compacted clay liner in minimizing advective and diffusive transport into the underlying groundwater system is emphasized from results presented herein. Without it, the lagoon would not have functioned properly.

Fig. 6. Variation of chloride leachate concentration during the service of the lagoon.

Summary and conclusions

An evaluation of a 1.5 mm HDPE geomembrane used as a liner in a leachate lagoon for 14 years has been presented. The number of defects (holes, patches, and cracks) and wrinkles, the “waterbed” nature of the geomembrane at the time of decommissioning, and the chloride diffusion profile through the clay suggest that the geomembrane likely did not perform its design function for very long. The amount of antioxidant measured via the standard OIT indicated very short times, generally less than 7 min. The OIT also indicated that antioxidants were almost completely consumed for the exposed part of the geomembrane, with an OIT value of about 1 min. This suggests that some oxidation may have already occurred in this part of the geomembrane as confirmed by the low values measured for the tensile break properties and the stress cracking resistance. The relatively low permeation coefficients inferred for a high crystallinity geomembrane relative to that for a modern lower crystallinity geomembrane suggests that diffusion in an intact geomembrane may decrease with time if the degree of crystallinity increased with time. The results also suggest that the chloride measured in the compacted clay had migrated essentially through the different defects present in the geomembrane liner and that the geomembrane ceased to effectively perform its barrier function at a relatively short time after installation. However, because the compacted clay liner was 3 m thick and chloride had only diffused 1.7 m, failure of the geomembrane did not cause any adverse impact on the groundwater.

Acknowledgements

The study was financially supported by the Natural Sciences and Engineering Research Council of Canada

(NSERC) and the Centre for Research in Earth and Space Technology (CRESTech). The authors appreciate the help of Dr. G.Y. Hsuan of GRI, Drexel University, U.S.A., and Mr. S. Usher (Gartner Lee Ltd.) for performing some of the initial tests and (or) for providing valuable comments on the data and observations reported in this paper.

References

- Adams M.W., and Wagner, N. 2000. Evaluating physical property integrity of a geomembrane used at a wastewater treatment facility for 11 years. *Geotechnical Fabrics Report*, **18**(7): 36–39.
- Basnett, C., and Brungard, M. 1992. The clay desiccation of a landfill composite lining system. *Geotechnical Fabrics Report*, **38**: 38–41.
- Corser P., Pellicer, J., and Cranston, M. 1992. Observations on the long term performance of composite clay liners and covers. *Geotechnical Fabrics Report*, **10**(8): 6–16.
- Eith, A.W., and Koerner, G.R. 1997. Assessment of HDPE geomembrane performance in a municipal waste landfill double liner system after eight years of service. *Geotextiles and Geomembranes*, **15**(4–6): 277–287.
- Hrapovic, L. 2001. Laboratory study of intrinsic degradation of organic pollutants in compacted clayey soil. Ph.D. thesis, The University of Western Ontario, London, Ont., 300 p.
- Hsuan, Y.G. 1999. Database of field incidents used to establish HDPE geomembrane stress crack resistance specifications. *Geotextiles and Geomembranes*, **18**(1): 1–22.
- Hsuan, Y.G. 2000. Laboratory index and performance tests of polyolefin geomembranes. *In Proceedings of EuroGeo 2000*, Bologna, Italy, 15–18 October, pp. 132–147.
- Hsuan, Y.G., and Koerner, R.M. 1995. Long term durability of HDPE geomembrane: Part I – Depletion of antioxidant. Geosynthetic Research Institute, Drexel University, Philadelphia, Pa., GRI Report 16, 35 pp.

- Hsuan, Y.G., and Koerner, R.M. 1997. GRI finalizes its first specification. *Geotechnical Fabrics Report*, **15**(5): 17–20.
- Hsuan, Y.G., and Koerner, R.M. 1998. Antioxidant depletion lifetime in high density polyethylene geomembranes. *Journal of Geotechnical and Geoenvironmental Engineering*, ASCE, **124**(6): 532–541.
- Hsuan, Y.G., Lord, A.E., Jr., and Koerner, R.M. 1991. Effects of outdoor exposure on high density polyethylene geomembrane. *In Geosynthetics '91 Conference Proceedings*, Atlanta, Ga., Industrial Fabrics Association International (IFAI), St. Paul, Minn., pp. 287–302.
- Koerner, R.M. 1999. *Designing with geosynthetics*, 4th ed., Prentice-Hall Inc., N.J., 761 pp.
- Lake, C.B. 2000. Contaminant transport through geosynthetic clay liners and composite liner system. Ph.D. thesis, The University of Western Ontario, London, Ont., 408 pp.
- Montgomery, J.H., and Welkom, L.M. 1990. *Groundwater chemicals desk reference*, Lewis Publishers Inc., Chelsea, Mich.
- Narejo, D.B., Koerner, R.M., and Wilson-Fahmy, R.F. 1996. Puncture protection of geomembranes Part II: Experimental. *Geosynthetics International*, **3**(5): 629–653.
- Naylor, T.deV. 1989. Permeation properties. *In Comprehensive polymer science*. Edited by C. Booth and C. Price. Pergamon Press, Oxford, England, Vol. 2, pp. 643–668.
- Peggs, I.D., and Carlson, D.S. 1989. Stress cracking of polyethylene geomembrane: Field experience. *In Durability and aging of geosynthetics*. Edited by R.M. Koerner. Elsevier Applied Science, London, pp. 195–211.
- Rogers, C.E. 1985. Permeation of gases and vapors in polymers, Chapter 2. *In Polymer permeability*. Edited by J. Comyn. Elsevier Applied Science, London, pp. 11–73.
- Rollin, A.L., Mlynarek, J., and Zanescu, A. 1994. Performance changes in aged in-situ HDPE geomembrane. *In Landfilling of waste: Barriers*, Edited by T.H. Christensen, R. Cossu, and R. Stegmann. E & F N Spon (Routledge) London. pp. 915–924.
- Rowe, R.K. 1998. Geosynthetics and the minimization of contaminant migration through barrier systems beneath solid waste. *In Proceedings of the 6th International Conference on Geosynthetics*, Atlanta, Ga., 25–29 March. Industrial Fabrics Association International (IFAI), St. Paul, Minn., Vol. 1, pp. 27–103.
- Rowe, R.K. 2001. Liner systems, Chapter 25. *In Geotechnical and Geoenvironmental Engineering Handbook*, Kluwer Academic Publishing, Norwell, Mass., pp. 739–788.
- Rowe, R.K., and Lake, C.B. 1997. Program LEAK — A program for calculating leakage through holes in a geomembrane in composite liners. The University of Western Ontario, London, Ont.
- Rowe, R.K., Hrapovic, L., and Kosaric, N. 1995a. Diffusion of chloride and dichloromethane through an HDPE geomembrane. *Geosynthetics International*, **2**(3): 507–536.
- Rowe, R.K., Quigley, R.M., and Booker, J.R. 1995b. *Clayey barrier systems for waste disposal facilities*. E & FN Spon (Chapman & Hall), London, 390 pp.
- Rowe, R.K., Hsuan, Y.G., Lake, C.B., Sangam, P., and Usher, S. 1998. Evaluation of a composite (geomembrane/clay) liner for a lagoon after 14 years of use. *In Proceedings of the 6th International Conference on Geosynthetics*, Atlanta, Ga., 25–29 March. Industrial Fabrics Association International (IFAI), St. Paul, Minn., Vol. 1, pp. 191–196.
- Rowe, R.K., Booker, J.R., and Fraser, J. 1999. POLLUTE v6.3.6 — 1D Pollutant migration through a non-homogeneous soil. GAEA Technologies Ltd., Whitby, Ont.
- Sangam, H.P. 2001. Performance of HDPE geomembrane liners in landfill applications, Ph.D. dissertation, The University of Western Ontario, London, Ont., 394 pp.
- Sangam, H.P., and Rowe, R.K. 2001. Migration of dilute aqueous organic pollutants through HDPE geomembranes. *Geotextiles and Geomembranes*, **19**(6): 329–357.
- Schmidt, R.K., Young, C., and Helwitt, J. 1984. Long term field performance of geomembranes — fifteen years experience. *In Proceedings of the International Conference on Geomembranes*, Denver, Colo., Industrial Fabrics Association International (IFAI), St. Paul, Minn., Vol. II, pp. 173–187.
- Tognon, A.R., Rowe, R.K., and Moore, I.D. 2000. Geomembrane strain observed in large-scale testing of protection layers. *Journal of Geotechnical and Geoenvironmental Engineering*, **126**(12): 1194–1208.